Published by
NIGERIAN SOCIETY OF PHYSICAL SCIENCES
Available online @ https://journal.nsps.org.ng/index.php/jnsps

J. Nig. Soc. Phys. Sci. 6 (2024) 1972

Journal of the Nigerian Society of Physical Sciences

Dynamical and optimal control analysis of lymphatic filariasis and buruli ulcer co-infection

Helen Olaronke Edogbanya[a,*], Emmanuel Sabastine[a], Rosalio G. Artes Jr.[b], Regimar A. Rasid[b]

[a]*Department of Mathematics, Federal University Lokoja, Nigeria*
[b]*Mindanao State University Tawi-Tawi College of Technology and Oceanography, Philipines*

Abstract

This study delves into the dynamics of lymphatic filariasis and buruli ulcer coinfection, two overlooked yet impactful tropical diseases. With lymphatic filariasis, commonly referred to as elephantiasis, and buruli ulcer, a chronic affliction caused by mycobacterium ulcerans, both posing significant health challenges, understanding their interaction is crucial. Utilizing a mathematical model, this research aims to analyze the dynamics of this coinfection, elucidating its complexities. The study establishes the local asymptotic stability of the disease-free equilibrium and calculates the basic reproduction number using the next generation matrix. It uncovers transcritical and backward bifurcation phenomena within the model. Additionally, the integration of time-dependent controls enables the exploration of optimal disease management strategies. Numerical simulations highlight the efficacy of employing a comprehensive approach, utilizing all available controls simultaneously, as the most effective strategy for disease control. These findings underscore the importance of integrated interventions in combating lymphatic filariasis and buruli ulcer coinfection, offering valuable insights for public health policymakers and practitioners.

DOI:10.46481/jnsps.2024.1972

Keywords: Neglected tropical disease, Mathematical model, Lymphatic filariasis, Buruli ulcer, Optimal control

Article History :
Received: 15 January 2024
Received in revised form: 20 June 2024
Accepted for publication: 20 August 2024
Published: 08 September 2024

Communicated by: P. Thakur

1. Introduction

Neglected Tropical Diseases (NTDs) represent a diverse array of infectious diseases commonly observed in tropical and subtropical regions worldwide, as reported by Receveur *et al.* [1] & Durojaye *et al.* [2]. This group of infectious diseases primarily impacts impoverished and vulnerable populations, encompassing 20 conditions such as Buruli Ulcer (BU), snakebite envenoming, onchocerciasis (river blindness), Chagas disease, dengue, and chikungunya, dracunculiasis (guinea-worm disease), lymphatic filariasis (LF), trachoma, and others, as outlined by George *et al.* [3]. NTDs are usually caused by viruses, bacteria, protozoa, or helminths and are not viewed as priorities in terms of public health according to George *et al.* [3], Hassoun Cosler [4] & Gyorkos *et al.* [5]. According to the findings of Sun and Amon [6], early detection plays a crucial role in preventing and treating the disease, NTDs have affected about 2 billion people (see Refs. [7]), with 206,155 reported death cases (discussed in [8]). Recent studies conducted by Refs. [9–11] have demonstrated that when non-NTDs such as Hepatitis B Virus (HBV), Human Immunodeficiency Virus (HIV), Tuberculosis (TB), Malaria, and COVID-19 coexist with NTDs, the

*Corresponding author: Tel.: +234-803-597-7988.
Email address: helen.edogbanya@fulokoja.edu.ng (Helen Olaronke Edogbanya)

Figure 1: Response to treatment following integrative medicine in elephantiasis (lymphedema) due to lymphatic filariasis ([31]) (Response to treatment).

severity of the diseases increases.

Similarly, other studies by Camelo *et al.* [12] and Azonvide *et al.* [13] have shown that co-infections between NTDs also occur. For example, co-infections of Schistosoma and Leishmania, as well as Buruli ulcer and Filariasis, have been documented, although little is known about this phenomenon. In particular, Azonvide *et al.* [13] reported that residents in BU-endemic areas are usually prone to Filariasis. In several localities within Ghana where BU is endemic, cases OF LF induced by Wuchereria bancrofti worm have been recorded. Therefore, Azonvide et al. [13] suggested exploring the co-infection of Buruli Ulcer (BU) with Filariasis in the treatment of BU.

LF is an NT Ds popularly known as elephantiasis, which is a major cause of morbidity in the developing world. Medeiros *et al* [14] have demonstrated that after Leprosy, Lymphatic Filariasis (LF) is the second-largest cause of disability and deformity globally. The transmission of LF involves infected mosquitoes depositing filarial parasites into the lymphatic system of healthy individuals, as outlined by Refs. [15, 16]. The filarial parasites responsible for LF are Wuchereria bancrofti, Brugia malayi and B. timori [15]. Furthermore, it is clarified that Wuchereria bancrofti is the prevailing species, responsible for 90 percent of the estimated 70 million cases of LF worldwide [16, 17]. The Global Program to Eliminate Lymphatic Filariasis (GPELF) was launched in 2000 by the World Health Organisation (WHO) to end the transmission of LF through the yearly administration of a large-scale treatment called Mass Drug Administration (MDA) and reduce the suffering induced by LF via the provision of morbidity management and disability prevention (MMDP) [18]. Figure 1 vividly demonstrates the treatment response of patients afflicted with LF, offering valuable insights into therapeutic outcomes and disease management.

Buruli ulcer, another NTD highlighted in the research by Coutts *et al.* [19] and Boakye-Appiah *et al.* [20], is an acute and debilitating skin condition caused by Mycobacterium Ulcerans. Multiple investigations document instances of Buruli Ulcer (BU) spanning 33 nations, with a notable prevalence in West Africa and Southeastern Australia [21–23]. Recent reports estimated that there are more than 67,000 people infected with BU worldwide [20]. Despite the global increase in BU infection, the precise epidemiology and mode of transmission of BU remain evasive. The majority of BU infections in West Africa are attributed to amphibians, fishes, mollusks, beetles, and water bugs [24, 25]. Conversely, in Australia, possums are identified as the natural reservoir of BU [26]. Recently, Refs. [20, 27] explored the efficacy of a combination of clarithromycin and rifampicin in treating BU infection, although these antibiotics are not free from side effects [28, 29]. Figure 2 illustrates the characteristic signs of BU before treatment initiation and the notable progress observed throughout the treatment process. These visual representations depict the evolution of lesions, healing rates, and overall improvement, providing valuable insights into the efficacy of therapeutic interventions for managing BU infection.

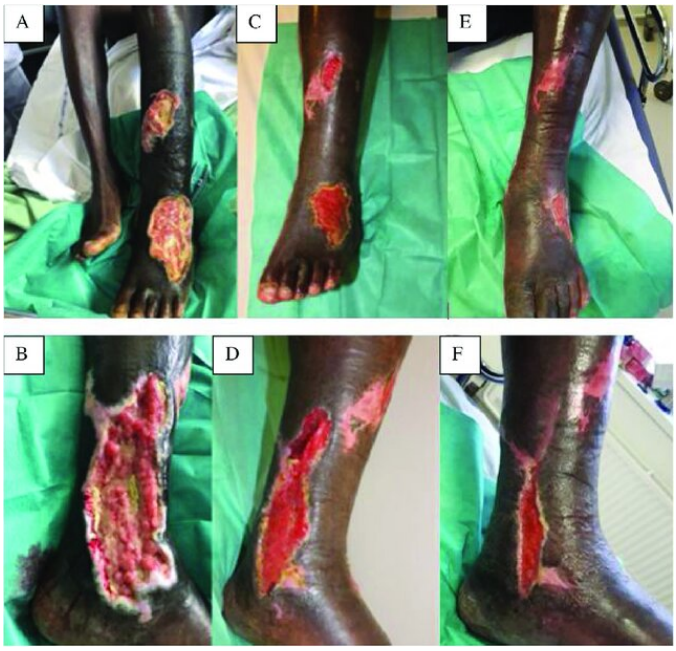

Figure 2: Leg infected with Mycobacterium ulcerans (Buruli ulcer) with undermining edges. Images A and B show the lesions at the time of presentation to the Department of Dermatology; images C and D show the lesions after 6 months of treatment; images E and F show the lesions after 9 months of treatment ([32]).

Mathematical models are used to improve the understanding of how to stop the transmission of infectious diseases. With the help of these models, relevant parameters and controls that affected the spread of infectious diseases in the past and those that will influence the spread in the future are determined and considered to make a well-informed decision. Some of the recent mathematical models for LF are found in Solonga *et al.* [30], Darmawati *et al.* [33], Rycht´ar *et al.* [34], Febiriana *et al.* [35] and Alshehri *et al.* [36]. Similarly, Edholm *et al.* [37], Momoh *et al.* [38], Khan *et al.* [39] , Clark and Bern [40] and Fandio *et al.* [41] have also studied the transmission dynamics of BU. The objective of this paper is to construct and assess a

mathematical model delineating the co-infection dynamics of two neglected tropical diseases, namely Lymphatic Filariasis and Buruli Ulcer.

As far as my understanding extends, there is currently a gap in mathematical research concerning the co-infection of Lymphatic Filariasis (LF) and Buruli Ulcer (BU). This study seeks to fill a critical knowledge gap by conducting a comprehensive mathematical analysis of the intricate dynamics and interactions between Lymphatic Filariasis (LF) and Buruli Ulcer (BU). Its primary objective is to meticulously explore effective strategies for combating the coinfection of LF and BU. Through this investigation, the study aims to generate valuable insights and recommendations to significantly enhance disease management and control efforts within the realm of neglected tropical diseases. By shedding light on these complexities, the research aims to deepen our understanding of LF and BU coinfection dynamics and provide actionable guidance for the development of impactful public health interventions.

The rest of the paper is structured as follows: Section 2 deals with the model formulation and analysis, the optimal control model is presented in section 3, section 4 deals with the numerical simulation while the conclusion of the study is presented in section 5.

2. Model formulation

A mathematical model that couples the models in Khan *et al.* [39] and Salonga *et al.* [30], is used to describe the transmission dynamics of *LF* and *BU* co-infection. The proposed model is made up of the population of humans, mosquitoes, water bugs and mycobacterium ulcerans. The total human population $N(t)$ is subdivided into five compartments, namely susceptible class $S(t)$, exposed individuals infected with *LF* only class $L_1(t)$, infectious individuals with *LF* infection only class $L_2(t)$, infectious *BU* infected humans only class $B(t)$ and the class of those infected with both *LF*, *BU* and $C(t)$ the co-infection class.
Thus

$$N(t) = S(t) + L_1(t) + L_2(t) + B(t) + C(t). \tag{1}$$

The susceptible mosquitoes $M_1(t)$ and the *LF* infected mosquito $M_2(t)$ made up the mosquitoes population $M(t)$. Similarly, the total water bugs population $W(t)$ is made of two subpopulations, namely, the susceptible water bugs $W_1(t)$ and the *BU* infected water bugs $W_2(t)$. Lastly, the concentration of mycobacterium ulcerans in the environment is denoted by $E(t)$.
The assumptions below were considered in the proposed model.

1 Only healthy individuals are recruited into the human population.
2 The shedding of mycobacterium ulcerans from individuals in $B(t)$ increases the concentration of mycobacterium ulceran in the environment
3 The susceptible humans $S(t)$ get infected with *LF* and *BU* at the rate $\lambda_l S$ and $\lambda_b S$ respectively such that $\lambda_l = \dfrac{\beta_2 M_2}{N}$, and $\lambda_b = \beta_b W_2 + \beta_e E$.
4 The mosquitoes and water bugs gets infected with *LF* and *BU* at the rate $\lambda_m M_1$ and $\lambda_w W_1$, respectively. The forces of infection λ_m and λ_w are given by

$$\lambda_m = \frac{\beta_1 (L_2 + \eta_1 C)}{N}, \quad \text{and} \quad \lambda_w = \beta_w (B + \eta_2 C),$$

respectively.
5 Individuals in L_2 class and B class gets infected with *BU* and *LF* and progresses to the co-infected class $C(t)$ at the rate $\lambda_v L_2$ and $\lambda_s B$ respectively. Where

$$\lambda_s = \frac{\beta_3 M_2}{N} \quad \text{and} \quad \lambda_v = \beta_v W_2.$$

Based on the above mentioned assumptions, Figure 3 and Table 1 illustrate the transmission dynamics of a two co-infected $NT - Ds$, namely, *LF* and *BU* is governed by the following first order non-linear system of ordinary differential equations.

$$\frac{dS}{dt} = \Pi_h + (\gamma_1 L_1 + \gamma_2 L_2) q - (\lambda_l + \lambda_b + \mu_h) S, \tag{2}$$

$$\frac{dL_1}{dt} = \lambda_l S - (\gamma_1 q + \theta + \mu_h) L_1, \tag{3}$$

$$\frac{dL_2}{dt} = \theta L_1 - (\gamma_2 q + \mu_h) L_2, \tag{4}$$

$$\frac{dB}{dt} = \lambda_b S - (\mu_h + \delta_b + \lambda_s) B, \tag{5}$$

$$\frac{dC}{dt} = \lambda_v L_2 + \lambda_s B - (\mu_h + \delta_c) C, \tag{6}$$

$$\frac{dM_1}{dt} = \Pi_m - (\lambda_m + \mu_m) M_1, \tag{7}$$

$$\frac{dM_2}{dt} = \lambda_m M_1 - \mu_m M_2, \tag{8}$$

$$\frac{dW_1}{dt} = \Pi_w - (\lambda_w + \mu_w) W_1, \tag{9}$$

$$\frac{dW_2}{dt} = \lambda_w W_1 - \mu_w W_2, \tag{10}$$

$$\frac{dE}{dt} = B\tau - E\mu_e. \tag{11}$$

2.1. Disease free equilibrium and computation of R_0

Let the disease free equilibrium be denoted by Σ_0, such that its component are given by:

$$\Sigma_0 (S^*, L_1^*, L_2^*, B^*, C^*, M_1^*, M_2^*, W_1^*, W_2^*, E^*) = \left(\frac{\Pi_h}{\mu_h}, 0, 0, 0, 0, \frac{\Pi_m}{\mu_m}, 0, \frac{\Pi_w}{\mu_w}, 0, 0\right).$$

Table 1: Description and estimation of parameters for the model. Notes: The parameters listed as 1-5 and 16 in the table below were sourced from Salonga *et al.* [30], while all remaining data were cited from Khan *et al.* [39].

Parameter	Description	Estimated value
$\Pi_{(h,m,w)}$	Recruitment rates into humans, mosquitoes and water bugs population	$(100,\ 4.227\times10^{4},\ 1000)$
$\mu_{(h,m,w)}$	Natural death rates for humans, mosquitoes and water bugs population	$(4\times10^{-5},\ 0.123,\ 0.0714)$
$\delta_{(l,b,c)}$	Disease induced death rate for individuals suffering from LF, BU and dual infections	$(0.001,\ 0.07,\ 0.7)$
$\gamma_{(1,2)}$	Treatment rate for individuals in L_1 and L_2 compartments	$(0.0615,\ 0.0014)$
q	Treatment coverage	0.619
β_1	Transmission coefficient of LF from infected humans to susceptible mosquitoes	0.232582
β_2	Transmission coefficient of LF from infected mosquitoes to susceptible humans	0.0000113
β_3	LF transmission coefficient from infected mosquitoes to BU infected humans	0.000113
β_b	BU transmission coefficient from infected water bugs to susceptible humans	1×10^{-7}
β_w	BU transmission coefficient from infected humans to to susceptible water bugs	3×10^{-6}
β_v	BU transmission coefficient from infected water bugs to LF infected humans.	2×10^{-7}
β_e	BU transmission coefficient from the Mycobacterium ulcerans in the environment to susceptible humans	5×10^{-9}
η_1	The modification parameter associated with the decrease in LF transmission to susceptible mosquitoes by individuals in C compartment	1.2
η_2	The modification parameter associated with the decrease in BU transmission to susceptible mosquitoes by individuals in C compartment	1.2
τ	Shedding rate of Mycobacterium ulcerans into the environment	0.0714
μ_e	Natural death rate of the Mycobacterium ulcerans in the environment	0.123
θ	Progression rate from L_1 to L_2 compartment	0.37

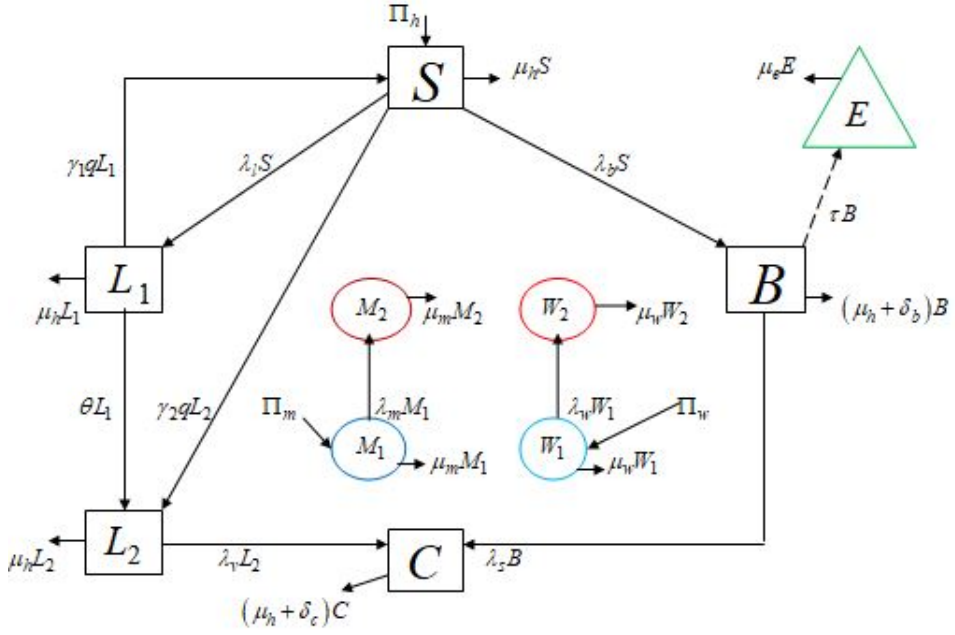

Figure 3: Schematic representation of the model (model diagram).

Computing the Reproduction number using the next generation method to have

$$F=\begin{bmatrix} 0 & 0 & 0 & 0 & \beta_2 & 0 & 0\\ 0 & 0 & 0 & 0 & 0 & 0 & 0\\ 0 & 0 & 0 & 0 & 0 & \frac{\beta_b\Pi_h}{\mu_h} & \frac{\beta_e\Pi_h}{\mu_h}\\ 0 & 0 & 0 & 0 & 0 & 0 & 0\\ 0 & \frac{\beta_1\mu_h\Pi_m}{\Pi_h\mu_m} & 0 & \frac{\beta_1\eta_1\mu_h\Pi_m}{\Pi_h\mu_m} & 0 & 0 & 0\\ 0 & 0 & \frac{\beta_w\Pi_w}{\mu_w} & \frac{\beta_w\eta_2\Pi_w}{\mu_w} & 0 & 0 & 0\\ 0 & 0 & 0 & 0 & 0 & 0 & 0 \end{bmatrix},$$

$$Q=\begin{bmatrix} k_1 & 0 & 0 & 0 & 0 & 0 & 0\\ -\theta & k_2 & 0 & 0 & 0 & 0 & 0\\ 0 & 0 & k_3 & 0 & 0 & 0 & 0\\ 0 & 0 & 0 & k_4 & 0 & 0 & 0\\ 0 & 0 & 0 & 0 & \mu_m & 0 & 0\\ 0 & 0 & 0 & 0 & 0 & \mu_w & 0\\ 0 & 0 & -\tau & 0 & 0 & 0 & \mu_e \end{bmatrix}, \tag{12}$$

to be the matrices for the new infection term and the transition terms respectively. Then,

$$R_0=\rho(FQ^{-1})=max\left\{R_0^L\ ,\ R_0^B\right\}. \tag{13}$$

where

$$R_0^L = \sqrt{R_1 R_2}, \quad R_0^B = \frac{R_e + \sqrt{4R_bR_w + R_e^2}}{2}, \quad R_1 = \frac{\beta_1\mu_h\Pi_m\theta}{\Pi_h\mu_m k_2 k_1},$$

$$R_2 = \frac{\beta_2}{\mu_m}, \quad R_w = \frac{\beta_w\Pi_w}{\mu_w k_3}, R_e = \frac{\beta_e\Pi_h\tau}{\mu_h\mu_e k_3}, \quad R_b = \frac{\beta_b\Pi_h}{\mu_h\mu_w},$$

$k_1 = \mu_h + \theta + \gamma_1 q$, $k_2 = \mu_h + \gamma_2 q$, $k_3 = \mu_h + \delta_b$, $k_4 = \mu_h + \delta_c$.

2.2. Local stability of DFE

Theorem 2.1. *Whenever $R_0 < 1$, the DFE of equations (2)-(11) is locally asymptotically stable and unstable if $R_0 > 1$*

Proof. The Jacobian matrix of equations (2)-(11) evaluated at DFE is given by

$$J(DFE) = \begin{bmatrix}
-\mu_h & \gamma_1 q & \gamma_2 q & 0 & 0 & 0 & -\beta_2 & 0 & -\frac{\beta_b\Pi_h}{\mu_h} & -\frac{\beta_e\Pi_h}{\mu_h} \\
0 & -k_1 & 0 & 0 & 0 & 0 & \beta_2 & 0 & 0 & 0 \\
0 & \theta & -k_2 & 0 & 0 & 0 & 0 & 0 & 0 & 0 \\
0 & 0 & 0 & -k_3 & 0 & 0 & 0 & 0 & \frac{\beta_b\Pi_h}{\mu_h} & \frac{\beta_e\Pi_h}{\mu_h} \\
0 & 0 & 0 & 0 & -k_4 & 0 & 0 & 0 & 0 & 0 \\
0 & 0 & -\frac{\beta_1\mu_h\Pi_m}{\Pi_h\mu_m} & 0 & -\frac{\beta_1\eta_1\mu_h\Pi_m}{\Pi_h\mu_m} & -\mu_m & 0 & 0 & 0 & 0 \\
0 & 0 & \frac{\beta_1\mu_h\Pi_m}{\Pi_h\mu_m} & 0 & \frac{\beta_1\eta_1\mu_h\Pi_m}{\Pi_h\mu_m} & 0 & -\mu_m & 0 & 0 & 0 \\
0 & 0 & 0 & -\frac{\beta_w\Pi_w}{\mu_w} & -\frac{\beta_w\eta_2\Pi_w}{\mu_w} & 0 & 0 & -\mu_w & 0 & 0 \\
0 & 0 & 0 & \frac{\beta_w\Pi_w}{\mu_w} & \frac{\beta_w\eta_2\Pi_w}{\mu_w} & 0 & 0 & 0 & -\mu_w & 0 \\
0 & 0 & 0 & \tau & 0 & 0 & 0 & 0 & 0 & -\mu_e.
\end{bmatrix} \tag{14}$$

From equation (14), it is readily seen that $\lambda_1 = -\mu_m, \lambda_2 = -\mu_w, \lambda_3 = -\mu_e$.

$$\lambda^7 + a_1\lambda^6 + a_2\lambda^5 + a_3\lambda^4 + a_4\lambda^3 + a_5\lambda^2 + a_6\lambda + a_7 = 0, \tag{15}$$

where

$$a_1 = \mu_e + \mu_w + \mu_m + k_1 + k_2 + k_3 + k_4, \tag{16}$$

$$a_2 = X_0 + (k_1 + \mu_m + k_2 + k_4)(k_2 + \mu_e + \mu_w) + (k_1 + \mu_m)(k_2 + k_4) + k_1\mu_m, \tag{17}$$

$$a_3 = X_0(k_1 + \mu_m + k_2 + k_4) + X_1(\mu_e + \mu_m) + \mu_e\mu_w k_3(1 - R_bR_w - R_e) + X_2, \tag{18}$$

$$a_4 = X_1X_0 + X_2(\mu_m + \mu_e) + \mu_m\mu_e k_3(1 - R_bR_w - R_e) + \mu_m k_1 k_2 k_4(1 - R_1R_2), \tag{19}$$

$$a_5 = X_2X_0 + \mu_w\mu_e K_3 x_1(1 - R_bR_w - R_e) + k_1k_2k_4\mu_m(k_3 + \mu_e + \mu_m)(1 - R_1R_2), \tag{20}$$

$$a_6 = K_1K_2K_4\mu_m X_0(1 - R_1R_2) + \mu_w\mu_e k_3 X_2(1 - R_bR_w - R_e), \tag{21}$$

$$a_7 = \mu_e\mu_m\mu_w k_1k_2k_3k_4(1 - R_bR_w - R_e)(1 - R_1R_2), \tag{22}$$

$$X_0 = k_3[\mu_3(1 - R_e) + \mu_w(1 - R_bR_w)] + \mu_e\mu_w, \tag{23}$$

$$X_1 = (k_1 + k_2 + k_4)\mu + (k_2 + k_4)k_1 + k_2k_4, \tag{24}$$

$$X_2 = \mu_m\{k_1[k_4 + k_2(1 - R_1R_2)] + k_2k_4\} + k_1k_2k_4. \tag{25}$$

It is readily seen that a_1 and a_2 are positive since all the model parameters are positive. Similarly, $a_i > 0$ for all $i = 3, ..., 7$ provided $R_0 < 1$. Following Chu *et al.* [42], equation (15) will have seven negative eigenvalues if a_i and m_i are positive for all $i = 1, \ldots, 7$, where

$$m_1 = a_1, \quad m_2 = \begin{bmatrix} a_1 & 1 \\ a_3 & a_2 \end{bmatrix}, \quad m_3 = \begin{bmatrix} a_1 & 1 & 0 \\ a_3 & a_2 & a_1 \\ 0 & 0 & a_3 \end{bmatrix}, \tag{26}$$

$$m_4 = \begin{bmatrix} a_1 & 1 & 0 & 0 \\ a_3 & a_2 & a_1 & 0 \\ 0 & a_4 & a_3 & a_2 \\ 0 & 0 & 0 & a_4 \end{bmatrix},$$

$$m_5 = \begin{bmatrix} a_1 & 1 & 0 & 0 & 0 \\ a_3 & a_2 & a_1 & 1 & 0 \\ a_5 & a_4 & a_3 & a_2 & a_1 \\ 0 & 0 & a_5 & a_4 & a_3 \\ 0 & 0 & 0 & 0 & a_5 \end{bmatrix}, \tag{27}$$

$$m_6 = \begin{bmatrix} a_1 & 1 & 0 & 0 & 0 & 0 \\ a_3 & a_2 & a_1 & 1 & 0 & 0 \\ a_5 & a_4 & a_3 & a_2 & a_1 & 1 \\ 0 & a_6 & a_5 & a_4 & a_3 & a_2 \\ 0 & 0 & 0 & a_6 & a_5 & a_4 \\ 0 & 0 & 0 & 0 & 0 & a_6 \end{bmatrix}, \tag{28}$$

$$m_7 = \begin{bmatrix} a_1 & 1 & 0 & 0 & 0 & 0 & 0 \\ a_3 & a_2 & a_1 & 1 & 0 & 0 & 0 \\ a_5 & a_4 & a_3 & a_2 & a_1 & 1 & 0 \\ a_7 & a_6 & a_5 & a_4 & a_3 & a_2 & a_1 \\ 0 & 0 & a_7 & a_6 & a_5 & a_4 & a_3 \\ 0 & 0 & 0 & 0 & a_7 & a_6 & a_5 \\ 0 & 0 & 0 & 0 & 0 & 0 & a_7 \end{bmatrix}. \tag{29}$$

With the help of Maple 18 software, it is readily seen that $m_i > 0$. Thus, equation (15) has all its eigenvalue to be negative. Furthermore, the model equations (2)-(11) is said to be locally asymptotically stable whenever $R_0 < 1$. □

2.3. Existence of transcritical and backward bifurcation

Using the centre manifold theory described in Castillo-Chavez and Song (2004) to explore the existence of forward and backward bifurcation. Then, system in equations (2)-(11) is written as

$$f_1 = \Pi_h + (x_2\gamma_1 + x_3\gamma_2)q - \left(\frac{\beta_2 x_7}{\sum_{i=1}^5 x_i} + x_9\beta_b + x_{10}\beta_e + \mu_h\right)x_1, \tag{30}$$

$$f_2 = \frac{\beta_2 x_7 x_1}{\sum_{i=1}^5 x_i} - k_1x_2, \tag{31}$$

$$f_3 = \theta x_2 - k_2x_3, \tag{32}$$

$$f_4 = (x_9\beta_b + x_{10}\beta_e)x_1 - x_4k_3, \tag{33}$$

$$f_5 = \frac{x_4\beta_3 x_7}{\sum_{i=1}^5 x_i} - x_5k_4 + \beta_v x_9 x_3, \tag{34}$$

$$f_6 = \Pi_m - \left(\frac{\beta_1 (x_5\eta_1 + x_3)}{\sum_{i=1}^{5} x_i} + \mu_m\right) x_6, \tag{35}$$

$$f_7 = \frac{\beta_1 (x_5\eta_1 + x_3)\, x_6}{\sum_{i=1}^{5}} - x_7\mu_m, \tag{36}$$

$$f_8 = \Pi_w - (\beta_w (x_5\eta_2 + x_4) + \mu_w)\, x_8, \tag{37}$$

$$f_9 = \beta_w (x_5\eta_2 + x_4)\, x_8 - x_9\mu_w, \tag{38}$$

$$f_{10} = \tau\, x_4 - x_{10}\mu_e, \tag{39}$$

where $N = \sum_{i=1}^{5} x_i$. The component of the right and left eigenvectors of the Jacobian matrix given by equation (14) with the assumption that $\beta_2 = \beta_2^* = \mu_m$ are expressed, respectively, as

$$\begin{aligned} &V_1 = V_4 = V_6 = V_8 = V_9 = V_{10} = 0,\\ &V_2 = \frac{\theta V_3}{k_1}, \quad V_5 = \frac{\theta \Pi_m V_3 \beta_1 \beta_2 \eta_1 \mu_h}{k_1 k_4 \Pi_h {\mu_m}^2},\\ &V_7 = \frac{\beta_2 \theta V_3}{k_1 \mu_m}. \end{aligned} \tag{40}$$

Note that V_i, for$i = 1, 2, \cdots, 10$ are the right eigen-vectors.

$$\begin{aligned} Z_1 &= \frac{Z_3 \left(q k_1 \Pi_h \gamma_2 {\mu_m}^2 + q \Pi_m \beta_1 \beta_2 \gamma_1 \mu_h - k_1 \Pi_m \beta_1 \beta_2 \mu_h\right)}{k_1 \Pi_h \mu_h {\mu_m}^2},\\ Z_2 &= \frac{\beta_2 \beta_1 \mu_h \Pi_m Z_3}{k_1 \Pi_h {\mu_m}^2},\\ Z_6 &= -\frac{\beta_1 \mu_h \Pi_m Z_3}{\Pi_h {\mu_m}^2},\\ Z_7 &= -\frac{\beta_1 \mu_h \Pi_m Z_3}{\Pi_h {\mu_m}^2},\\ Z_4 &= Z_8 = Z_9 = Z_{10} = 0. \end{aligned} \tag{41}$$

Note that Z_i, for $i = 1, 2, \cdots, 10$ are the left eigen-vectors.

Next, use

$$a = \sum_{h,i,j=1}^{10} V_h Z_i Z_j \frac{\partial^2 f_h}{\partial x_i x_j}, b = \sum_{h,i,j=1}^{10} V_h Z_i \frac{\partial^2 f_h}{\partial x_i \beta_2^*}$$

to get

$$\begin{aligned} a &= -2\frac{{\beta_1}^2 \mu_h V_3 {W_3}^2 {\Pi_m}^2 \theta {\beta_2}^2 \mu_h (Q-1)}{K_1 {\mu_m}^4 {\Pi_h}^3},\\ b &= \frac{W_3 \beta_2 \theta V_3 \mu_h \Pi_m}{K_1 \Pi_h {\mu_m}^2}, \end{aligned} \tag{42}$$

where
$Q = \frac{K_1\mu_m(q\gamma_2\mu_m+\beta_1\mu_h+2\,\mu_h\mu_m)\Pi_h+\beta_1\beta_2\mu_h\Pi_m(q\gamma_1+2\,\mu_h)}{K_1\Pi_m\beta_1\beta_2\mu_h}$.
According to the centre manifold theory, the sign of a and b that determines the direction of the bifurcation. Oviously, $b > 0$ while $a < 0$ if $Q > 1$ and $a > 0$ if $Q < 1$.Based on Theorem 4.1 in Castillo-Chavez and Song [43], the following result is established.

Theorem 2.2. *The model equations (2)-(11) undergoes a forward (transcritical) bifurcation if $Q > 1$ and a backward (subcritical) bifurcation if $Q < 1$.*

Epidemiologically, the existence of backward bifurcation suggests that $R_0 < 1$ is not sufficient to ensure that the disease dies out.

3. Optimal control model

The modification of model equations (2)-(11) is given in this section by introducing three time-dependent controls denoted by $u_1(t), u_2(t)$ and $u_3(t)$. The controls $u_1(t)$ and $u_3(t)$ denote the effort of preventing LF and BU respectively. The treatment of either LF and BU is denoted by $u_2(t)$. The optimal control model is governed by the following system of first order differential equations:

$$\begin{aligned} g_1 &= \frac{dS}{dt} = \Pi_h + (\gamma_1 L_1 + \gamma_2 L_2)\, u_2\\ &\quad - (\lambda_l(1-u_1) + \lambda_b(1-u_3) + \mu_h)\, S,\\ g_2 &= \frac{dL_1}{dt} = \lambda_l(1-u_1)S - (\gamma_1 u_2 + \theta + \mu_h)\, L_1,\\ g_3 &= \frac{dL_2}{dt} = \theta L_1 - (\gamma_2 u_2 + \mu_h)\, L_2,\\ g_4 &= \frac{dB}{dt} = \lambda_b(1-u_3)S - (k_3 + u_2)\, B,\\ g_5 &= \frac{dC}{dt} = \lambda_v L_2 + \lambda_s B - (k_4 + u_2)\, C,\\ g_6 &= \frac{dM_1}{dt} = \Pi_m - (\lambda_m(1-u_1) + \mu_m)\, M_1,\\ g_7 &= \frac{dM_2}{dt} = \lambda_m(1-u_1)M_1 - \mu_m M_2,\\ g_8 &= \frac{dW_1}{dt} = \Pi_w - (\lambda_w(1-u_3) + \mu_w)\, W_1,\\ g_9 &= \frac{dW_2}{dt} = \lambda_w(1-u_3)W_1 - \mu_w W_2,\\ g_{10} &= \frac{dE}{dt} = B\tau - E\mu_e \end{aligned} \tag{43}$$

The objective functional to be minimized is given by

$$J(u_1,\ u_2,\ u_3) = \int_0^T d_1 L_2 + d_2 B + d_3 C + \frac{1}{2}\sum_{i=1}^{3} A_i u_i^2\, dt. \tag{44}$$

The purpose of $J(u_1,\ u_2,\ u_3)$ is to minimize the number of all infectious human population and the cost of implementing the three time dependent controls. Hence, the optimal triple control $u = (u_1,\ u_2,\ u_3)$ such that

$$J(u_1^*,\ u_2^*,\ u_3^*) = min_{u_1^*,\ u_2^*,\ u_3^*\ \in u} J(u_1,\ u_2,\ u_3), \tag{45}$$

is sought for such that

$$\begin{aligned} u = \{u_i : u_i &\text{ is measurable and } 0 \leqq u_i(t) \leq 1\\ &\text{for } i = 1, 2, 3,\ \ t \in [0,\ T]\} \end{aligned}$$

is the control set.

Given that the optimal control problem involves three time-dependent controls, Table 2 above outlines the interventions under consideration.

Table 2: Sample strategies.

Strategy type	Strategy	Control conditions
Single Strategies	Prevention of LF	Strategy I $(u_1 \neq 0, u_2 = 0, u_3 = 0)$
	Treatment of LF and BU	Strategy II $(u_1 = 0, u_2 \neq 0, u_3 = 0)$
	Prevention of BU	Strategy III $(u_1 = 0, u_2 = 0, u_3 \neq 0)$
Double Strategies	Prevention of LF + Treatment of LF and BU	Strategy IV $(u_1 \neq 0, u_2 \neq 0, u_3 = 0)$
	Prevention of LF + Treatment of LF and BU	Strategy V $(u_1 \neq 0, u_2 = 0, u_3 \neq 0)$
	Prevention of BU + Treatment of LF and BU	Strategy VI $(u_1 = 0, u_2 \neq 0, u_3 \neq 0)$
Triple Strategy	Prevention of LF + Prevention of BU + Treatment of LF and BU	Strategy VII $(u_1 \neq 0, u_2 \neq 0, u_3 \neq 0)$
Without Controls	Strategy VIII	$(u_1 = 0, u_2 = 0, u_3 = 0)$

The Pontryagin's Maximum Principle is used to convert the optimality system $g_i, i = 1, ..., 10$ and equation (44) into a problem of minimizing the Hamiltonian H, defined by

$$H = d_1 L_2 + d_2 B + d_3 C + \frac{1}{2}\sum_{i=1}^{3} A_i u_i^2 + \sum_{i=1}^{10} \chi_i g_i. \tag{46}$$

Theorem 3.1. *There exists an optimal control triple* (u_1^*, u_2^*, u_3^*) *and a corresponding state solution* $S^*, L_1^*, L_2^*, B^*, C^*, M_1^*, M_2^*, W_1^*, W_2^*$, *and* E^* *that minimizes* $J(u_1, u_2, u_3)$ *over* u. *Furthermore, there exist adjoint functions* $\chi_1, \ldots, \chi_{10}$ *satisfying*

$$\begin{aligned}
\frac{d\chi_1}{dt} &= -\chi_1\left(\frac{\beta_2 M_2(1-u_1)S}{N^2} - \frac{\beta_2 M_2(1-u_1)}{N} \right.\\
&\quad \left. - (E\beta_e + W_2\beta_b)(1-u_3) - \mu_h\right)\\
&\quad - \chi_2\left(-\frac{\beta_2 M_2(1-u_1)S}{N^2} + \frac{\beta_2 M_2(1-u_1)}{N}\right)\\
&\quad - \chi_4\left(E\beta_e + W_2\beta_b\right)(1-u_3) + \frac{\chi_5\beta_3 M_2 B}{N^2}\\
&\quad - \frac{\chi_6\beta_1(\eta_1 C + L_2)(1-u_1)M_1}{N^2}\\
&\quad + \frac{\chi_7\beta_1(\eta_1 C + L_2)(1-u_1)M_1}{N^2},
\end{aligned} \tag{47}$$

$$\begin{aligned}
\frac{d\chi_2}{dt} &= \frac{M_1(u_1-1)(\eta_1 C + L_2)(\chi_6-\chi_7)\beta_1 + \beta_2 S M_2(\chi_1-\chi_2)u_1}{N^2}\\
&\quad - \left((-\gamma_1 u_2 - \mu_h)\chi_2 + u_2\chi_1\gamma_1 + \chi_3\theta\right),
\end{aligned} \tag{48}$$

$$\begin{aligned}
\frac{d\chi_3}{dt} &= \frac{M_1(C\eta_1 - N + L_2)(\chi_6-\chi_7)(u_1-1)\beta_1 + \Xi_1}{N^2}\\
&\quad - W_2\beta_v\chi_5 - \chi_1\gamma_2 u_2 + \chi_3\gamma_2 u_2 + \chi_3\mu_h - d_1,
\end{aligned} \tag{49}$$

$$\begin{aligned}
\Xi_1 &= (\beta_2 S(\chi_1-\chi_2)u_1 - \beta_2 S(\chi_1-\chi_2) + B\chi_5\beta_3)M_2,\\
\frac{d\chi_4}{dt} &= \frac{-\chi_5\beta_3 M_2 N + M_1(C\eta_1 + L_2)(\chi_6-\chi_7)(u_1-1)\beta_1 + \Xi_2}{N^2}\\
&\quad + \frac{M_2 B\chi_5\beta_3}{N^2} - W_1\beta_w(\chi_8-\chi_9)u_3 + W_1\beta_w(\chi_8-\chi_9)\\
&\quad + \chi_4(K_3 + u_2) - \chi_{10}\tau - d_2,
\end{aligned} \tag{50}$$

$$\begin{aligned}
\Xi_2 &= (\beta_2 S(\chi_1-\chi_2)u_1 - \beta_2 S(\chi_1-\chi_2))M_2,\\
\frac{d\chi_5}{dt} &= \frac{(-S(u_1-1)(\chi_2-\chi_1)\beta_2 + B\chi_5\beta_3)M_2 + \Xi_3}{N^2}\\
&\quad + \frac{\beta_1(u_1-1)M_1(\chi_6-\chi_7)((C-N)\eta_1 + L_2)}{N^2}\\
&\quad - \beta_w\eta_2(u_3-1)W_1(\chi_8-\chi_9),
\end{aligned} \tag{51}$$

$$\begin{aligned}
\Xi_3 &= ((K_4 + u_2)\chi_5 - d_3)N^2,\\
\frac{d\chi_6}{dt} &= \frac{-(\chi_6-\chi_7)(u_1-1)(\eta_1 C + L_2)\beta_1 + N\mu_m\chi_6}{N}\\
\frac{d\chi_7}{dt} &= \frac{-S(\chi_1-\chi_2)(u_1-1)\beta_2 - B\chi_5\beta_3 + \chi_7\mu_m N}{N}\\
\frac{d\chi_8}{dt} &= -(\chi_8-\chi_9)(u_3-1)(C\eta_2 + B)\beta_w + \mu_w\chi_8\\
\frac{d\chi_9}{dt} &= -S(\chi_1-\chi_4)(-1+u_3)\beta_b - \chi_5\beta_v L_2 + \mu_w\chi_9\\
\frac{d\chi_{10}}{dt} &= -S(\chi_1-\chi_4)(-1+u_3)\beta_e + \mu_e\chi_{10}.
\end{aligned} \tag{52}$$

With the transversality conditions $\chi_i(T) = 0$, *for all* $i = 1, ..., 10$ *such that*

$$\begin{aligned}
u_1^* &= \min\{u_{1max}, \max\{0, u_1^+\}\},\\
u_2^* &= \min\{u_{2max}, \max\{0, u_2^+\}\},\\
u_3^* &= \min\{u_{3max}, \max\{0, u_3^+\}\},
\end{aligned} \tag{53}$$

and

$$\begin{aligned}
u_1^+ &= -\frac{M_1(\chi_6-\chi_7)(C\eta_1 + L_2)\beta_1 + \beta_2 S M_2(\chi_1-\chi_2)}{A_1 N},\\
u_2^+ &= \frac{-L_1(\chi_1-\chi_2)\gamma_1 - L_2(\chi_1-\chi_3)\gamma_2 + \chi_4 B + \chi_5 C}{A_2},\\
u_3^+ &= -\frac{-W_1(\chi_9-\chi_8)(C\eta_2 + B)\beta_w + S(\chi_1-\chi_4)(E\beta_e + W_2\beta_b)}{A_3}.
\end{aligned} \tag{54}$$

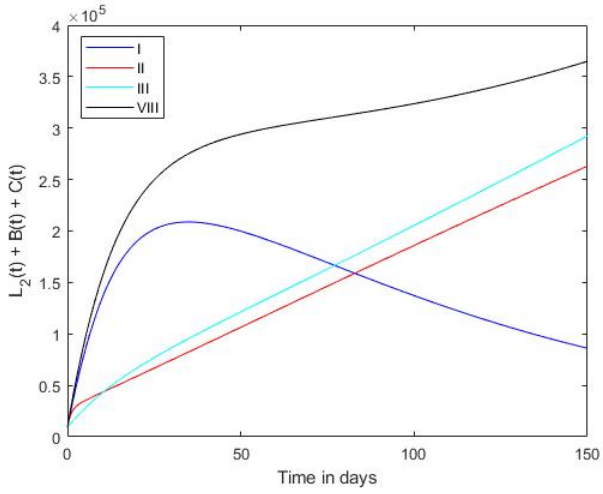

Figure 4: Effect of single strategies on the total infectious population.

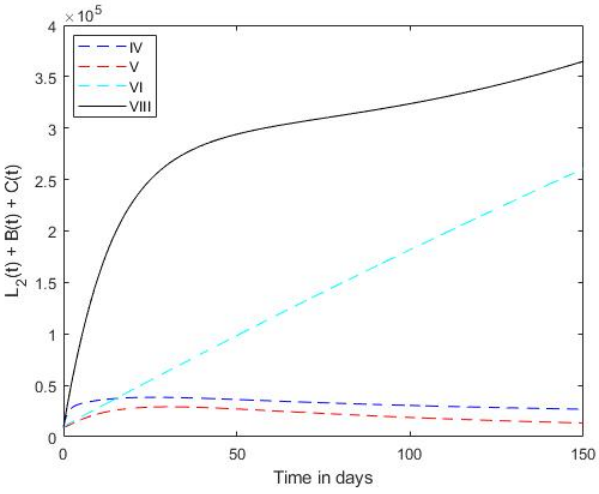

Figure 6: Effect of double strategies on the total infectious population.

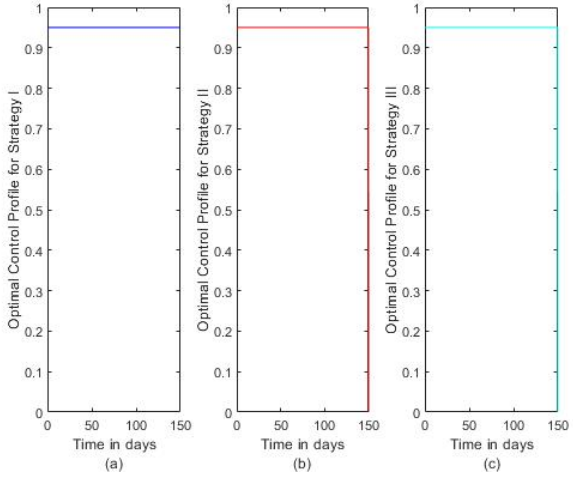

Figure 5: Optimal control profile for single strategies.

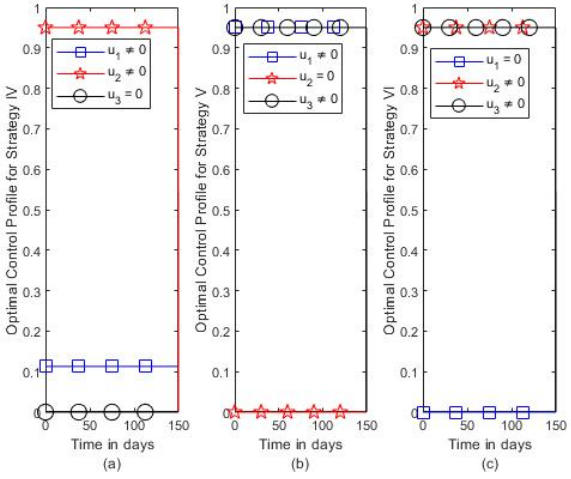

Figure 7: Optimal control profile for double strategies.

Proof. To obtain equation (52), the partial derivatives of the Hamiltonian H given by equation (46) with respect to each of the state variables are computed as follows

$$\begin{aligned}
\frac{d\chi_1}{dt} &= -\frac{\partial H}{\partial S} && \chi_1(T) = 0\\
\frac{d\chi_2}{dt} &= -\frac{\partial H}{\partial L_1} && \chi_2(T) = 0\\
&\vdots \quad \dots \quad \vdots && \vdots\\
\frac{d\chi_{10}}{dt} &= -\frac{\partial H}{\partial E} && \chi_{10}(T) = 0.
\end{aligned} \tag{55}$$

Next, the partial derivatives of equation (46) with respect to the control variables $(u_1,\ u_2,\ u_3)$ and equating it to zero to get

$$\frac{\partial H}{\partial u_1} = A_1u_1 + \frac{\beta_2 S M_2(\chi_1-\chi_2) - \beta_1 M_1(\chi_7-\chi_6)(C\eta_1+L_2)}{N} = 0,$$

$$\begin{aligned}
\frac{\partial H}{\partial u_2} &= A_2u_2 + \chi_1(L_1\gamma_1 + L_2\gamma_2) - \chi_2\gamma_1L_1\\
&\quad - \chi_3\gamma_2L_2 - \chi_4B - \chi_5C = 0,
\end{aligned} \tag{56}$$

$$\begin{aligned}
\frac{\partial H}{\partial u_3} &= A_3u_3 + W_1(\chi_8-\chi_9)(C\eta_2+B)\beta_w\\
&\quad - (E\beta_e + W_2\beta_b)(\chi_4-\chi_1)S = 0.
\end{aligned} \tag{57}$$

The solution of equation (54) gives equation (56) and considering the bounds on the control, the characterizations of the controls are given by equation (53). □

4. Numerical simulation

To show the effect of the time dependent controls, the strategies outlined in Table 2 will be considered such that both diseases are persistent ($R_0^L = 1.5015 > 1$ and $R_0^L = 1.0119 > 1$). The simulation is performed by the software MATLAB 21.a

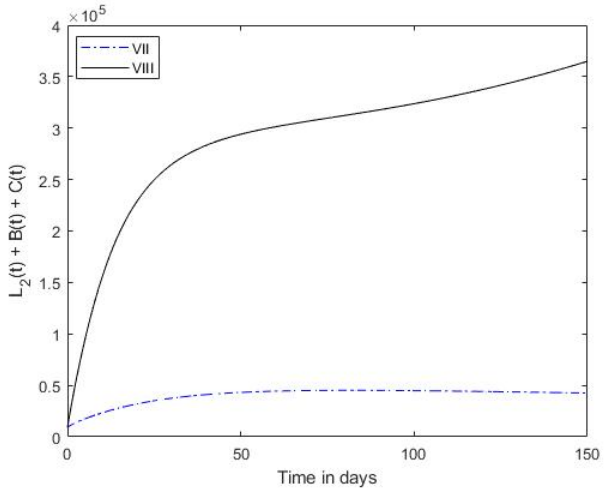

Figure 8: effect of triple strategy on the total infectious population.

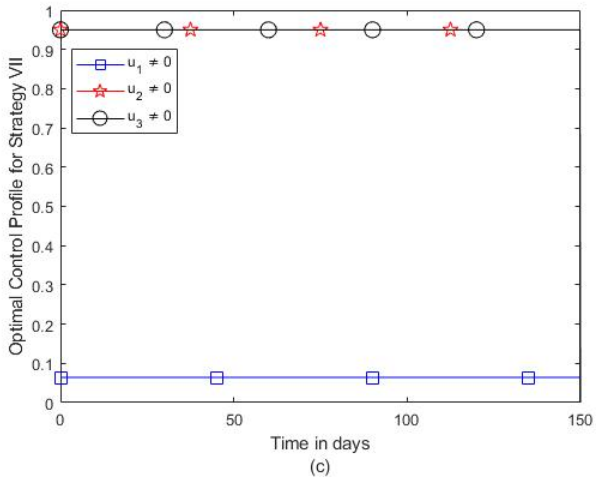

Figure 9: Optimal control profile for triple strategy.

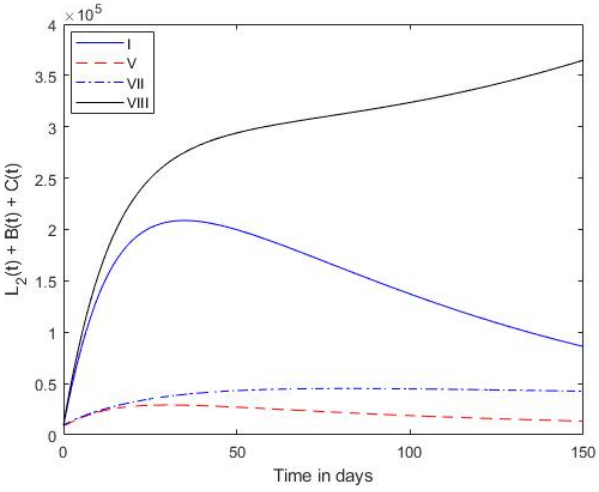

Figure 10: Comparison of strategies I, V, VII and VIII.

version using the forward backward sweep method of a fourth order Runge-Kutta iterative scheme outlined in Lenhart and Workman (2007). For the purpose of simulation, the values of parameter in Table 1, thta is the weight constants $d_1 = 1$, $d_2 = 210$, $d_3 = 300$, $A1 = 100$, $A2 = 50$, $A3 = 150$, and the initial population $S(0) = 2,490,000$, $L_1 = 5,000$, $L_2 = 2,450$, $B = 1,650, C = 1,000, M_1 = 3,399,000$, $M_2 = 1,000$, $W_1 = 10,000$, $W_2 = 4,000$ and , $E = 1,400,000$ are used. Note that this data were also gathered from Khan and Salonga *et al.* [30, 39].

Figure 4 illustrates the effects of implementing single strategies on the collective population of infectious humans ($L_2(t) + B(t) + C(t)$). As depicted in the figure, each single strategy implementation results in a notable reduction in the total infectious population compared to the absence of control (Strategy VIII). Notably, among the three strategies, only Strategy I consistently decreases the population $L_2(t) + B(t) + C(t)$, while the others show an upward trend. This observation underscores the effectiveness of Strategy I in minimizing $L_2(t) + B(t) + C(t)$.

Figure 5 demonstrates how the control of each single strategies should be applied to ensure that the goal of the objective function is satisfied. Figure 5a shows that the control for the prevention of LF (u_1) remains at the upper bound (0.95) for the simulation period of 150 days while the control for the prevention of BU(u_3) and treatment u_2 as depicted by Figure 5c & b are at upper bound but decreases to zero on the final day.

The effect of the double strategies on the population of all infectious humans are depicted in Figure 6. The figure shows that all the double strategies have less population of infectious humans compared to Strategy VIII (without control). This suggest that the application of any of the double strategies is of great importance in curbing the dual spread of LF and BU. It is obvious to note that among the three double strategies, Strategy V(that is the application of both u_1 and u_3) generates the least number of infectious human. Thus, it is considered to be the best double strategy.

The optimal control profile for each of the double strategies are displayed in Figure 7. The controls that made up Strategies V(u_1 and u_3) and VI (u_2 and u_3) remains at the upper bound while for Strategy IV, the control u_2 is at upper bound and that of u_1 remains at about 8% through out the simulation period of 150 days.

Figure 8 demonstrates the impact of implementing the triple strategy on the population of all infectious humans. It illustrates that the adoption of Strategy VII leads to a decrease in the number of all infectious individuals.

The implementation of the triple strategy is displayed by Figure 9. According to the figure, the controls u_2 and u_3 should be implemented optimally through out the simulation while 8% of the control u_1 should be used for a period of 150 days.

In order to identify the optimal strategy for minimizing the population of all infected humans, we conducted a comparison among the single control strategy (Strategy I), the double control strategy (Strategy II), and the triple strategy (Strategy VII). As depicted in Figure 10, it is evident that among the three

strategies, Strategy V results in the lowest number of infectious humans, followed by Strategy VII. Hence, we conclude that Strategy V stands as the superior strategy.

5. Conclusion

In this study, we have developed a mathematical model to elucidate the simultaneous spread of two neglected tropical diseases: Lymphatic Filariasis (LF) and Buruli Ulcer (BU).

1. The proposed model comprises a system of first-order nonlinear differential equations, encompassing ten compartments to comprehensively capture the dynamics of LF and BU co-infection.
2. Key findings from our analysis include:
   (a) The local asymptotic stability of the model is contingent upon the basic reproduction number (R_0), with stability observed when R_0 is below unity and instability when it exceeds unity.
   (b) The model demonstrates a transcritical bifurcation when the parameter Q exceeds 1, and a backward bifurcation occurs when Q is less than 1.
   (c) Numerical simulations indicate that the implementation of any of the three time-dependent controls results in a reduction in the joint spread of LF and BU.
   (d) Regarding optimal control strategies, our analysis reveals that Strategy I, focusing on preventing LF, emerges as the most effective single strategy. Additionally, Strategy V, which combines efforts in LF prevention and the treatment of both LF and BU, proves to be the best double strategy, surpassing expectations by outperforming the triple strategy approach.
3. These findings underscore the importance of targeted interventions in mitigating the burden of LF and BU co-infection, with implications for disease control and public health policy formulation.

References

[1] J. P. Receveur, A. Bauer, J. L. Pechal, S. Picq, M. Dogbe, H. R. Jordan & M. E. Benbow, "A need for null models in understanding disease transmission: the example of Mycobacterium ulcerans (Buruli ulcer disease)", FEMS Microbiology Reviews **45** (2002) 22. https://doi.org/10.1093/femsre/fuab045.

[2] A. B. Durojaye, O. J. Adedeji, O. M. Egbewande, A. A. Ibrahim, E. S. Oladipupo, R. O. Yusuf & Y. Babatunde, "Enhancing communication strategies in controlling neglected tropical diseases in Nigeria", Public Health Challenges **2** (2023) 1. https://onlinelibrary.wiley.com/doi/pdf/10.1002/puh2.100.

[3] N. S. George, S. C. David, M. Nabiryo, B. A. Sunday, O. F. Olanrewaju, Y. Yangaza & D. O. Shomuyiwa, "Addressing neglected tropical diseases in Africa: a health equity perspective", Global Health Research and Policy **8** (2003) 7. https://doi.org/10.1186/s41256-023-00314-1.

[4] N. Hassoun & L. Cosler, "Global health impact: A model to alleviate the burden and expand access to treatment of neglected tropical diseases", The American Journal of Tropical Medicine and Hygiene **108** (2023) 806. https://doi.org/10.4269%2Fajtmh.21-0583.

[5] T. Gyorkos, R. Nicholls, A. Montresor, A. Luciañez, M. Casapia, K. St-Denis & S. Joseph, "Eliminating morbidity caused by neglected tropical diseases by 2030", Revista Panamericana de Salud Pública **47** (2023) 8. https://doi.org/10.26633/RPSP.2023.16.

[6] N. Sun & J. J. Amon, "Addressing inequity: neglected tropical diseases and human rights", Health and human rights **20** (2018) 25. https://www.ncbi.nlm.nih.gov/pmc/articles/PMC6039727/.

[7] D. Engels & X. N. Zhou," Neglected tropical diseases: an effective global response to local poverty-related disease priorities", Infectious diseases of poverty **9** (2020) 17. https://doi.org/10.1186/s40249-020-0630-9.

[8] J. M. Kirigia & G. N. Mburugu, "The monetary value of human lives lost due to neglected tropical diseases in Africa.", Infectious Diseases of Poverty **6** (2017) 627. http://doi.org/10.1186/s40249-017-0379-y.

[9] L. Da Silva Santos, H. Wolff, F. Chappuis, P. Albajar-Viñas, M. Vitoria, N. T. Tran & L. Gétaz, "Coinfections between persistent parasitic neglected tropical diseases and viral infections among prisoners from Sub-Saharan Africa and Latin America", Journal of tropical medicine **1** (2018) 10. https://doi.org/10.1155/2018/7218534.

[10] E. H. Clark & C. Bern "Chagas disease in people with HIV: a narrative review", Tropical Medicine and Infectious Disease **6** (2021) 10. https://search.informit.org/doi/pdf/10.3316/informit.337139314382189.

[11] A. U. Pradhan, O. Uwishema, J. Wellington, P. Nisingizwe, V. D. Thambi, C. V. P. Onyeaka & H. Onyeaka, "Challenges of addressing neglected tropical diseases amidst the COVID-19 pandemic in Africa: a case of Chagas disease", Annals of Medicine and Surgery **81** (2022) 4. https://doi.org/10.1016/j.amsu.2022.104414

[12] G. M. A. Camelo, J. K. A. D. O. Silva, S. M. Geiger, M. N. Melo, & D. A. Negrão-Corrêa, "Schistosoma and Leishmania: An untold story of coinfection", Tropical Medicine and Infectious Disease **8** (2023) 14. https://search.informit.org/doi/pdf/10.3316/informit.410361205236780.

[13] C. L. Azonvide, T. Adjobimey, H. Sina & L. Baba-Moussa, "Characterization of the influence of Mansonella perstans co-infection on immunity.", Journal of Infectious Diseases and Immunity **14** (2022) 5. https://doi.org/10.5897/JIDI2022.0217.

[14] Z. M. Medeiros, A. V. Vieira, A. T. Xavier, G. S. Bezerra, M. D. F. C. Lopes, C. V. Bonfim, & A. M. Aguiar-Santos, "Lymphatic filariasis: A systematic review on morbidity and its repercussions in countries in the Americas", International Journal of Environmental Research and Public Health **19** (2021) 18. https://www.mdpi.com/1660-4601/19/1/316.

[15] S. K. Ghosh & P. K. Srivastava, "A new outlook in lymphatic filariasis elimination in India", in *Parasitology and Microbiology Research*, IntechOpen, India, 2020. https://www.intechopen.com/chapters/72005.

[16] T. willliams, M. J. Karim, S. Uddin, S. Jahan,... & L. A. Kelly-Hope, "Socio-economic and environmental factors associated with high lymphatic filariasis morbidity prevalence distribution in Bangladesh", PLOS Neglected Tropical Diseases **17** (2023) 16. https://doi.org/10.1016/S0001-8791(03)00044-7.

[17] S. Emmanuel, S. Sathasivam, M. K. M. Ali, T. J. Kee & Y. S. Ling, "Estimating the transmission dynamics of Dengue fever in subtropical Malaysia using SEIR model", Journal of Quality Measurement and Analysis **19** (2023) 45. https://journalarticle.ukm.my/22244/1/Paper4%20-.pdf.

[18] M. Edmiston, S. Atinbire, E. O. Mensah, E. Mensah, B. Alomatu, K. Asemanyi Mensah & S. Palmer, "Evaluating the availability and quality of services for lymphatic filariasis morbidity in Ghana", PLOS Neglected Tropical Diseases **17** (2023) 15. https://journals.plos.org/plosntds/article?id=10.1371/journal.pntd.0010805.

[19] S. P. Coutts, C. L. Lau, E. J. Field, M. J. Loftus & E. L. Tay, "Delays in patient presentation and diagnosis for Buruli ulcer (Mycobacterium ulcerans infection) in Victoria, Australia", Tropical Medicine and Infectious Disease **4** (2019) 10. https://doi.org/10.3390/tropicalmed4030100.

[20] J. Boakye-Appiah, B. Hall, R. Reljic & R. E. Simmonds, *Current Progress and Prospects for a Buruli Ulcer Vaccine*, Springer International Publishing, 2023, pp. 71-95. https://doi.org/10.1007/978-3-031-24355-4_5.

[21] A. J. Muleta, R. Lappan, T. P. Stinear & C. Greening, "Understanding the transmission of Mycobacterium ulcerans: A step towards controlling Buruli ulcer", PLoS Neglected Tropical Diseases **15** (2021) 21. https://journals.plos.org/plosntds/article?id=10.1371/journal.pntd.0009678.

[22] P. I. Otuh, "Identification of genetic relatedness of Mycobacterium ulcerans DNA from human and aquatic environmental samples: One Health approach to Buruli ulcer epidemiology", Journal of Sustainable Veterinary & Applied Sciences **4** (2023) 895. https://josvasmouau.com/wp-content/uploads/2023/07/14.-Otuh-2023-1.pdf.

[23] S. Muhi, J. Osowicki, D. O'Brien, P. D. Johnson, S. Pidot, M. Doerflinger & T. P. Stinear, "A human model of Buruli ulcer: The case for controlled human infection and considerations for selecting a Mycobacterium ulcerans challenge strain", PLOS Neglected Tropical Diseases **17** (2023) 17. https://journals.plos.org/plosntds/article?id=10.1371/journal.pntd.0011394.

[24] D. O. Konan, L. Mosi, G. Fokou, C. Dassi, C. A. Narh, C. Quaye, ... & B. Bonfoh, "Buruli ulcer in southern Côte D'ivoire: dynamic schemes of perception and interpretation of modes of transmission", Journal of Biosocial Science **51** (2019) 533. https://doi.org/10.1017/S0021932018000317.

[25] A. Leuenberger, B. V. Koné, R. T. N'krumah, D. Y. Koffi, B. Bonfoh, J. Utzinger & G. Pluschke, "Perceived water-related risk factors of Buruli ulcer in two villages of south-central Côte d'Ivoire. PLOS Neglected Tropical Diseases", PLOS Neglected Tropical Diseases **16** (2022) e0010927. journals.plos.org/plosntds/article?id=10.1371/journal.pntd.0010927.

[26] R. W. Xu, T. P. Stinear, P. D. Johnson & D. P. O'Brien, "Possum bites man: case of Buruli ulcer following possum bite", Medical Journal of Australia **216** (2022) 453. https://onlinelibrary.wiley.com/doi/pdf/10.5694/mja2.51505.

[27] L. Dhungel, M. E. Benbow & H. R. Jordan, "Linking the Mycobacterium ulcerans environment to Buruli ulcer disease: Progress and challenges", One health **13** (2021) 9. https://doi.org/10.1016/j.onehlt.2021.100311.

[28] S. Y. Aboagye, G. Kpeli, J. Tuffour & D. Yeboah-Manu, "Challenges associated with the treatment of Buruli ulcer", Journal of Leukocyte Biology **105** (2019) 242. https://doi.org/10.1002/jlb.mr0318-128.

[29] A. I. Abioye, O. J. Peter, H. A. Ogunseye, F. A. Oguntolu, T. A. Ayoola & A. O. Oladapo, "A fractional-order mathematical model for malaria and COVID-19 co-infection dynamics", Healthcare Analytics **4** (2023) 15. https://doi.org/10.1016/j.health.2023.100210.

[30] P. K. N. Salonga, V. M. P. Mendoza, R. G. Mendoza & V. Y. Belizario Jr, "A mathematical model of the dynamics of lymphatic filariasis in Caraga region, the Philippines", Royal Society Open Science **8** (2021) 24. https://royalsocietypublishing.org/doi/pdf/10.1098/rsos.201965.

[31] S. R. Narahari & A. B. Kanjarpane, "Public health systems research: evidence-based integrative medicine provides leadership in chronic care", Current Science **104** (2013) 696. https://www.researchgate.net/publication/288449016.

[32] L. Dupechez, P. Carvalho, V. Hebert, L. Marsollier, M. Eveillard, E. Marion & M. Kempf, "Senegal, a new potential endemic country for Buruli ulcer", International Journal of Infectious Diseases **89** (2019) 130. https://doi.org/10.1016/j.ijid.2019.09.020.

[33] D. Darmawati, M. Musafira, D. Ekawati, W. Nur, M. Muhlis & S. F. Azzahra, "Sensitivity, optimal control, and cost-effectiveness analysis of intervention strategies of filariasis", Jambura Journal of Mathematics **4** (2022) 76. https://doi.org/10.34312/jjom.v4i1.11766.

[34] J. Rychtár & D. Taylor, "A game-theoretic model of lymphatic filariasis prevention" PLoS Neglected Tropical Diseases **16** (2022) 18. https://journals.plos.org/plosntds/article?id=10.1371/journal.pntd.0010765.

[35] I. H. Febiriana, V. Adisaputri, P. Z. Kamalia & D. Aldila, "Impact of screening, treatment, and misdiagnose on lymphatic filariasis transmission: a mathematical model", Commun. Math. Biol. Neurosci. **2023** (2023) 67. https://doi.org/10.28919/cmbn/7983.

[36] A. Alshehri, Z. Shah & R. Jan, "Mathematical study of the dynamics of lymphatic filariasis infection via fractional-calculus", The European Physical Journal Plus **138** (2023) 15. https://link.springer.com/article/10.1140/epjp/s13360-023-03881-x.

[37] C. Edholm, B. Levy, A. Abebe, T. Marijani, S. Le Fevre, S. Lenhart & F. Nyabadza, "A risk-structured mathematical model of buruli ulcer disease in Ghana", in *Mathematics of Planet Earth*, H. Kaper, F. Roberts (Ed.), Springer, Cham., 2019, pp. 109-128. https://doi.org/10.1007/978-3-030-22044-0_5.

[38] A. A. Momoh, H. M. Abdullahi, N. G. Abimbola & A. I. Michael, "Modeling, optimal control of intervention strategies and cost effectiveness analysis for buruli ulcer model", Alexandria Engineering Journal **60** (2021) 2264. https://doi.org/10.1016/j.aej.2020.12.042.

[39] M. A. Khan, E. Bonyah, Y. X. Li, T. Muhammad & K. O. Okosun, "Mathematical modeling and optimal control strategies of Buruli ulcer in possum mammals", AIMS Mathematics **6** (2021) 9881. https://www.aimspress.com/aimspress-data/math/2021/9/PDF/math-06-09-572.pdf.

[40] E. H. Clark & C. Bern, "Chagas disease in people with HIV: a narrative review", Tropical Medicine and Infectious Disease **6** (2021) 10. https://search.informit.org/doi/pdf/10.3316/informit.337139314382189.

[41] R. Fandio, H. Abboubakar, H. P. E. Fouda & A. Kumar, "Mathematical modelling and projection of Buruli ulcer transmission dynamics using classical and fractional derivatives: A case study of Cameroon", Partial Differential Equations in Applied Mathematics **8** (2023) 100589. https://doi.org/10.1016/j.padiff.2023.100589.

[42] Y. M. Chu, M. Farhan, M. A. Khan, M. Y. Alshahrani, T. Muhammad, & S. Islam, "Mathematical modeling and stability analysis of Buruli ulcer in Possum mammals" Results in Physics **27** (2021) 104471. https://doi.org/10.1016/j.rinp.2021.104471.

[43] C. Castillo-Chavez, B. Song, "Dynamical models of tuberculosis and their applications", Mathematical Biosciences & Engineering **1** (2004) 361. http://doi.org/10.3934_mbe.2004.1.361.pdf.